Physics and Chemistry of the Earth 110 (2019) 149–156

Contents lists available at ScienceDirect

Physics and Chemistry of the Earth

journal homepage: www.elsevier.com/locate/pce

The higher, the cooler? Effects of building height on land surface temperatures in residential areas of Beijing

Zhong Zheng[a,b], Weiqi Zhou[a,b,*], Jingli Yan[a,b], Yuguo Qian[a], Jia Wang[a,b], Weifeng Li[a,b]

[a] State Key Laboratory of Urban and Regional Ecology, Research Center for Eco-Environmental Sciences, Chinese Academy of Sciences, Beijing, 100085, China
[b] University of Chinese Academy of Sciences, Beijing, 100049, China

ARTICLE INFO

Keywords:
UHI
Land surface temperature
Vertical structure
Building height
Building density
Beijing

ABSTRACT

Numerous studies have showed that landscape composition and configuration can significantly affect land surface temperature (LST). Most of these studies focus on the horizontal dimension of landscape structure. Few studies, however, have explored the effects of vertical dimension of urban landscape. This study aims to fill this gap. We focused on the residential landscapes in the central area of Beijing, and quantified the relationships between the vertical structure of buildings and LST. We delineated the boundaries of residential neighborhoods based on high resolution imagery, which were latterly used as the unit of statistical analysis. Building height, and proportional cover of buildings and vegetation were also mapped from high resolution imagery, with aid of digital maps. LST was retrieved from thermal band of TM imagery. We used Pearson correlation, partial correlation and ordinary least squares(OLS) regressions to quantify the relationships between these variables and LST. We found: 1) Land surface temperature varied greatly among residential neighborhoods, ranging from 53.5 °C to 37.0 °C, with a mean of 44.2 °C and a standard deviation of 2.4 °C. High-rise residential neighborhoods had the lowest LST, and mean LST decreased from low-rise to high-rise residential neighborhoods. 2) Building height, building density and vegetation coverage were all significantly correlated with LST. Building height and vegetation coverage has significantly negative effects on LST, but building density had a significantly positive one. 3) Among these variables, building height had greater impact on LST than the other two variables. These results have important implications for urban design and management.

1. Introduction

With the process of rapid urbanization, urban areas increased in size and population dramatically (Antrop, 2004; Grimmond, 2007; Seto et al., 2011). During this expansion, human activities reconstruct the natural environment and generate a series of environmental problems, such as the urban heat island (UHI)(Voogt and Oke, 2003; Oleson et al., 2011; Matsumoto et al., 2017). Meteorological observations have shown that temperatures in urban areas are higher than the surrounding rural areas (Oke, 1995; Voogt and Oke, 2003). High temperatures caused by the UHI have a negative effect on urban dwellers (Naughton et al., 2002; Duneier, 2006), and can also augment water and energy consumption during hot summer weather (Akbari et al., 2001; Guhathakurta and Gober, 2007). Additionally, the UHI effect may lead to the accumulation of air pollutants that cause great harm to humans, animals and plants in urban areas (Akbari et al., 2001; Basu and Ostro, 2008). For these reasons, UHI has attracted great attention by researchers and land managers who seek to understand and respond to ecological and health related issues.

Urban landscape pattern, and the change in the distribution of landscape components through time, have a significant effect on UHI. As a result of urbanization processes, urban land use/cover types continuously undergo tremendous modifications. Forests and croplands are replaced by impervious surfaces (e.g., roads, parking lots, rooftops and compacted soils), which alters their thermal properties and leads to the occurrence of UHI (Voogt and Oke, 2003; Basu and Ostro, 2008; Amiri et al., 2009; Zhou et al. 2011, 2017b; Kuang et al., 2015). Landscape configuration is also an important factor affecting the urban thermal environment, because landscape spatial patterns are closely related to the thermal environment of land surfaces (Wu, 2009; Zhou et al., 2011; Jiao et al., 2017). Changing the spatial arrangement of urban components may affect land surface energy distribution. For example, rearranging building structures and greenspaces, such as creating wind corridors in dense urban centers, could effectively mitigate the UHI (Gal

* Corresponding author. State Key Laboratory of Urban and Regional Ecology, Research Center for Eco-Environmental Sciences, Chinese Academy of Sciences, Beijing, 100085, China.
E-mail address: wzhou@rcees.ac.cn (W. Zhou).

https://doi.org/10.1016/j.pce.2019.01.008
Received 4 November 2018; Received in revised form 25 December 2018; Accepted 14 January 2019
Available online 18 January 2019
1474-7065/

and Unger, 2009; Hsieh and Huang, 2016). Furthermore, the size, shape, and fragmentation of landscape patches within the urban setting can have differential effects on land surface temperature (LST). For example, aggregated green spaces often have a greater cooling effect than fragmented green spaces with similar area (Zhou et al., 2011; Li et al., 2012; Su et al., 2014). Although these studies provide insights into how landscape composition and configuration affect the urban thermal environment, they are focused on the relationships between landscape patterns and UHI in the horizontal direction of two-dimensional space. In contrast, the number of studies that explore the dynamics of UHI within the three-dimensional urban landscape is relatively small (Chun and Guldmann, 2014; Berger et al., 2017).

Urban areas, with their artificial structures, are characterized by a unique three-dimensional landscape morphology that differs from natural ecosystems (Liu et al., 2017; Zhou et al., 2017a). Landscape pattern of two-dimensional space alone is inadequate in explaining the complex thermal phenomena occurring in urban areas. Complex urban three-dimensional components (mainly buildings and walls) also have a direct impact on the process of surface energy exchange, leading to differences in thermal environment between urban and natural land (Oke, 1981; Golany, 1996; Zhou et al., 2011). Previous studies have found that the high-rise buildings and narrow streets in urban locations can act as canyon structures. These canyons increase the absorption of solar radiation, and lead to the trapping of long-wave radiation from the ground. Walls of nearby buildings can act as windbreaks to reduce wind speed and prevent air flow from cooling the street canyons, contributing to further heating of the land surface (Oke, 1981, 1988; Forman, 1995; Unger, 2006). On the other hand, tall buildings can also provide large areas of shadow that reduce the solar radiation absorbed by ground, resulting in a lower LST (Nichol, 1996; Xiao et al., 2007). Through a combination of experimental measurements and numerical modeling, some studies about the relationship between three-dimensional landscapes and air temperature and LST have been conducted, mostly at the local scale. Oke (1988) established a numerical model to explain the relationship between height-width ratio(H/W)of street canyons and nocturnal UHI intensity in mid-latitude cities. Giridharan et al., (2005) found that an increased sky view factor (SVF) could lead to an increase in daytime UHI and a decrease in nocturnal UHI. As these geometric parameters integrating two-dimensional information are not enough to explore the direct effect of vertical dimensional factors on LST, height-related indicators have been typically chosen as the major parameters to characterize the three-dimensional landscape morphology (Guo et al., 2016; Cai et al., 2018). While these studies help explain the effect of urban three-dimensional structure on surface thermal environments at the local scale, studies on urban scale are relatively few. One of the major limitations has been the difficulty of obtaining high resolution three-dimensional information about urban landscapes at the scale of entire metropolitan areas.

Due to the rapid development of remote sensing technologies, it is now possible to acquire a large range of datasets with urban three-dimensional information. For example, aerial photography can provide details about urban structures for constructing three-dimensional models (Dubayah and Drake, 2000). Urban three-dimensional data can also be extracted using shadow cast by buildings based on high resolution satellite remote sensing data such as IKONOS and QUICKBIRD (Lee and Kim, 2013). Furthermore, the development of Light Detection And Ranging (LiDAR) sensors provides a rapid and highly accurate approach for acquiring three-dimensional information about buildings and vegetation in urban areas (Zhou et al., 2008; Sun and Salvaggio, 2013; Zhou, 2013; Yan et al., 2015). Together these technologies can provide data for use in investigating important relationships between the structural attributes of the urban landscape and UHI (Xiao et al., 2008; Su et al., 2014; Zhao et al., 2015).

This study used residential neighborhoods as unit of statistical analysis, and investigated the influence of residential landscapes and vertical structures on LST in the central area of Beijing. We used building height to describe the vertical structure of urban residential neighborhoods in the city. Building density and vegetation coverage were chosen as two important variables to represent landscape composition. The research was based on building height extracted from aerial orthophotos, high resolution satellite imagery and digital maps combined with land use data. The objectives of the study were to: (1) analyze the relationship between building height, building density, vegetation coverage and LST in residential neighborhoods, and (2) explore the relative importance of the influence of these three structural variables on LST. The study's findings can help illuminate the relationships between residential parameters of urban structural morphology and LST, and may have meaningful implications for urban planning and design.

2. Methods

2.1. Study area

Beijing, the capital of China, is located in the northern part of the North China Plain (39°28'–41°25'N, 115°25'–117°30'E). Beijing is the political, cultural and communication center of China, and it covers approximately 16,800 km^2 with a population of 21 million people. Its climate belongs to the warm temperate zone with a continental monsoon climate, hot summers and cold winters, with an annual average temperature of 12 °C and annual precipitation of approximately 600 mm. Beijing experienced a rapid urban expansion in recent decades. The associated increase in impervious surfaces aggravates the UHI effect (Qiao et al., 2014).

Beijing's development is a concentric expansion and it forms a ring-shaped pattern from the city center to its outskirts. Our study focused on the area within the 5th ring road of Beijing (Fig. 1), with an area of 666 km^2 and a population of 10 million people (Beijing Municipal Statistics Bureau, 2013). The area is located in the Beijing plain, the southeast part of Beijing municipality, with an elevation ranging from 20 to 60m. The flat terrain could reduce the impact of topography on land surface thermal environment. Our study focused on residential neighborhoods in this area because neighborhoods have the highest concentrations of residents and susceptibility to thermal environment. Vegetation and impervious surfaces with tall buildings of different heights are the dominant land cover types in this area and they both have effects on the land surface thermal environment (Qian et al., 2015).

2.2. Data

2.2.1. Land surface temperature

The land surface temperature (LST) data were derived from the thermal infrared (TIR) band (10.44–12.42 μm) of a Landsat-5 Thematic Mapper (TM) image, with a ground resolution of 120 m. The image was acquired at 10:27 am local time, on August 19, 2010, under clear atmospheric conditions. The image was obtained from the US geological survey (USGS) as Level-1 products, with radiometric and geometrical distortions corrected.

We retrieved the LST data using the radiance transfer equation (RTE) method, as detailed in (Zhou et al., 2014). First, we converted the digital number (DN) to top-of-atmosphere (TOA) radiance. We then converted the TOA radiance to surface-leaving radiance by removing the effects of atmosphere in the thermal region, using the equation detailed in Barsi et al., (2003). Finally, we calculated the apparent surface temperature (i.e., black-body temperature) based on the surface-leaving radiance, using the Landsat specific estimate of the Planck curve.

2.2.2. Building footprint data and building height

Building footprint (building boundaries) and number of building stories were extracted from a vector file of Baidu map data (map.baidu.

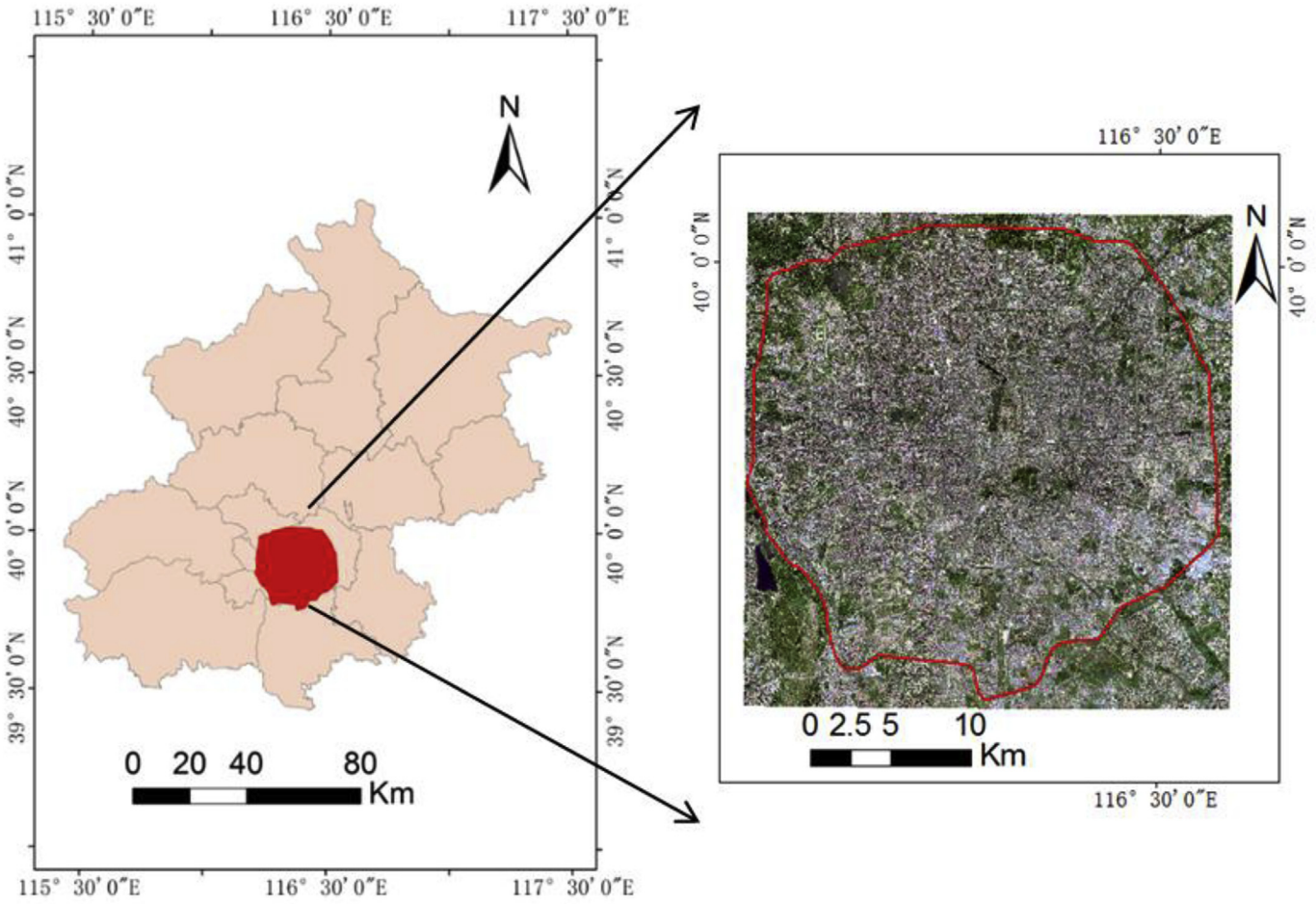

Fig. 1. Study Area: the region within the fifth ring road of Beijing, China.

com) in 2010. There are approximately 193,600 buildings in the study area. A considerable number of buildings have no story information, so the data were complemented through street view of Baidu map. In our study, story height was defined as 2.8m, the standard story height of residential buildings determined by Chinese Residential Building Code (Ministry of Construction of the People's Republic of China, 2005a).

According to the Chinese building classification mentioned in Code for Design of Civil Buildings (Ministry of Construction of the People's Republic of China, 2005b), the buildings were divided into four groups by the number of layers: low-rise buildings are lower than three stories; multi-story buildings between four and six stories; buildings that have between seven and nine stories are called middle-rise buildings; and high-rise buildings have ten or more stories.

2.2.3. High resolution land cover data

We used Advanced Land Observation Satellite (ALOS) imagery to obtain land cover data in the study area. The image was acquired on October 22, 2009 and it has one panchromatic band and four multispectral bands, with 2.5 m and 10 m spatial resolution, respectively. Then we pan-sharpened the image and obtained a multispectral image with a resolution of 2.5 m for land cover classification.

An object-based approach for was used to classify land cover. The object-based approach treats homogeneous pixels as one object and divides objects into different types. The approach makes full use of spatial information, texture and spectral information of high resolution panchromatic and multispectral data. The approach is more flexible and accurate than traditional pixel-based classification methods, especially for classifying images of high spatial resolution (Zhou et al., 2008). We identified four land cover classes: Vegetation, impervious surface (including buildings), water and bare soil. The overall accuracy of classification was 94.14% (kappa = 0.92), and the accuracy of greenspace was 95.4%.

2.3. Statistical analysis

2.3.1. Analytical unit and selected variables

To minimize the effects of other factors, such as artificial heat, we chose residential neighborhoods as the analytical unit to investigate the relationship between LST and vertical structure of the urban landscape. Boundaries of residential neighborhoods were delineated by on-screen digitization based on ALOS high resolution images with the assistance of Baidu Maps. We obtained 3852 residential neighborhoods inside the fifth ring road of Beijing. In order to match the LST data, we kept residential neighborhoods built before 2012 with an area greater than 14400 m² (pixel size of LST image). A total of 3033 residential neighborhoods was retained. The residential neighborhoods were then divided into four groups by the main types of buildings in them (Fig. 2 & Table 1).

The mean LST of each residential neighborhood was summarized and used for statistical analyses. To explore the relationship between urban three-dimensional structure and LST, we selected three parameters for residential neighborhoods. Mean building height was chosen as a quantitative index of vertical structure of buildings. Building density and vegetation coverage were chosen as factors expressing the horizontal pattern of buildings in residential neighborhoods (Table 2).

2.3.2. Correlation analysis and multiple linear regression

In order to analyze whether LST differed among residential

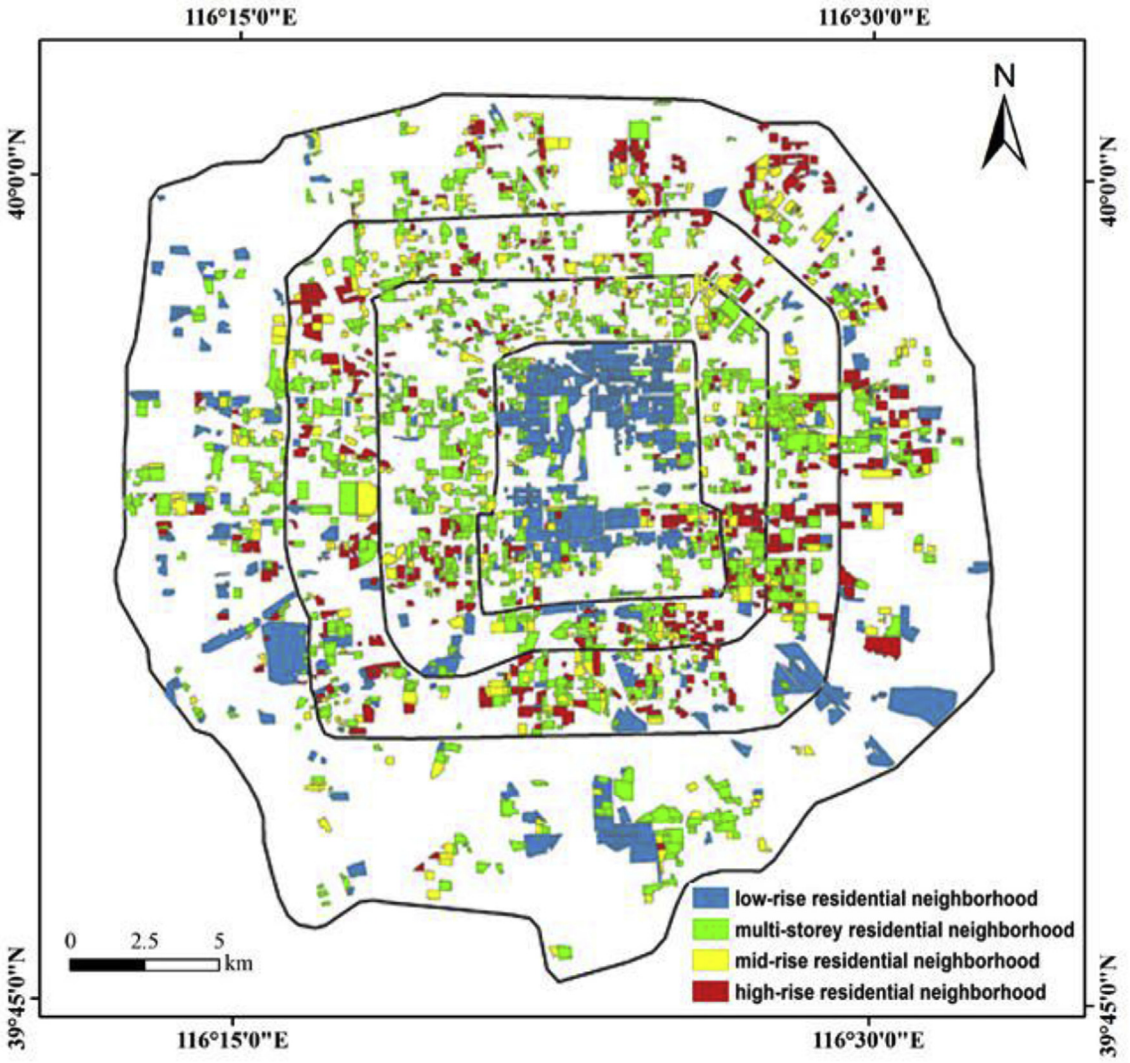

Fig. 2. Spatial distribution of residential neighborhoods with different building height in Beijing.

neighborhood types, we used Kruskal–Wallis one-way analysis of variance (ANOVA), a nonparametric method for comparing independent samples of different sizes. Then Pearson's correlation analysis was used to investigate correlation between LST and the three variables of mean building height, building density and vegetation coverage in residential neighborhoods. We further conducted partial Pearson's correlation analysis to investigate the relationship between LST and building height, after controlling for the effect of building density and vegetation coverage. To explore the relationships among LST and the three variables, ordinary least squares (OLS) regression was conducted. The dependent variable was LST in residential neighborhoods. All of the statistical methods mentioned were processed using SPSS22.

Table 2
Summary of LST and landscape variables of residential neighborhoods.

Variable names	Mean value	Std. Dev.
LST	44.2 ℃	2.4 ℃
Mean building height($\bar{H}$)	16.79m	12.70m
Building density(BD)	25.01%	10.60%
Vegetation coverage(VC)	22.80%	16.19%

3. Results

3.1. The 2D and 3D structure of buildings and vegetation in residential neighborhoods

Different residential neighborhoods have different landscape

Table 1
Classification of residential neighborhoods in terms of height of buildings.

Types	Stories	Number (percentage)	Area(ha) (percentage)
Low-rise residential neighborhoods	1–3	740(24.4%)	87.86(40.2%)
multi-story residential neighborhoods	4–6	1290(42.5%)	75.95(34.7%)
Mid-rise residential neighborhoods	7–9	414(13.6%)	23.33(10.6%)
high-rise residential neighborhoods	> 9	589(19.5%)	31.79(14.5%)

Table 3
Summary statistics for variables in the 4 types of residential neighborhoods in Beijing.

Residential type		Max	Min	Mean	SD
Low-rise residential neighborhoods	LST	53.5 °C	37.4 °C	44.9 °C	2.8 °C
	BD	66.82%	7.8%	27.48%	16.51%
	VC	89.62%	0%	21.39%	17.06%
Multi-story residential neighborhoods	LST	50.6 °C	39 °C	44.8 °C	2.0 °C
	BD	57.7%	8.7%	26.14%	7.52%
	VC	90.39%	0%	24.74%	16.9%
Mid-rise residential neighborhoods	LST	50.3 °C	38.9 °C	43.7 °C	2.0 °C
	BD	52.8%	10.96%	23.64%	6.78%
	VC	71.6%	0%	23.01%	14.84%
High-rise residential neighborhoods	LST	46.8 °C	37.0 °C	42.3 °C	1.7 °C
	BD	50.78%	6.74%	20.77%	7.12%
	VC	69.32%	0%	20.22%	13.7%

composition and three-dimensional configuration (Table 3). Building density of residential neighborhoods ranged from 7.8% to 66.82%, with a mean of 25.1% and a standard deviation of 10.6%. Mean height of buildings in different residential neighborhoods ranged from 2.8 m to 84 m, with a mean of 16.79 m and a standard deviation of 12.7 m. Vegetation coverage of residential neighborhoods varied greatly, ranging from 0% to 90.39%; the mean vegetation coverage was 22.8% and the standard deviation was 16.19%.

Table 4
Kruskal-Wallis ANOVA of LST in the four residential types and paired comparison test.

Group	Chi-sq	SE	Standardized Chi-sq	Sig
Global	583.19			0.00
a-b	11.918	40.365	0.295	0.768
b-c	453.087	49.42	9.168	0
c-d	519.295	56.127	9.252	0

a.Low-rise residential neighborhoods.
b.Multi-story residential neighborhoods.
c.Mid-rise residential neighborhoods.
d.High-rise residential neighborhoods.

Results from the Kruskal–Wallis one-way ANOVA showed significant differences in building density and vegetation coverage among the four types of residential neighborhoods. Building density in residential neighborhoods decreased from low-rise to high-rise residential neighborhoods. The variation of vegetation coverage had a decreasing tendency from multi-story to high-rise residential neighborhoods. The mean value of vegetation coverage in low-rise residential neighborhoods was 21.39%, higher than that in high-rise residential neighborhoods (20.22%), but lower than multi-story residential neighborhoods (24.74%) and middle-rise residential neighborhoods (23.01%). High-rise residential neighborhoods had both the lowest mean building

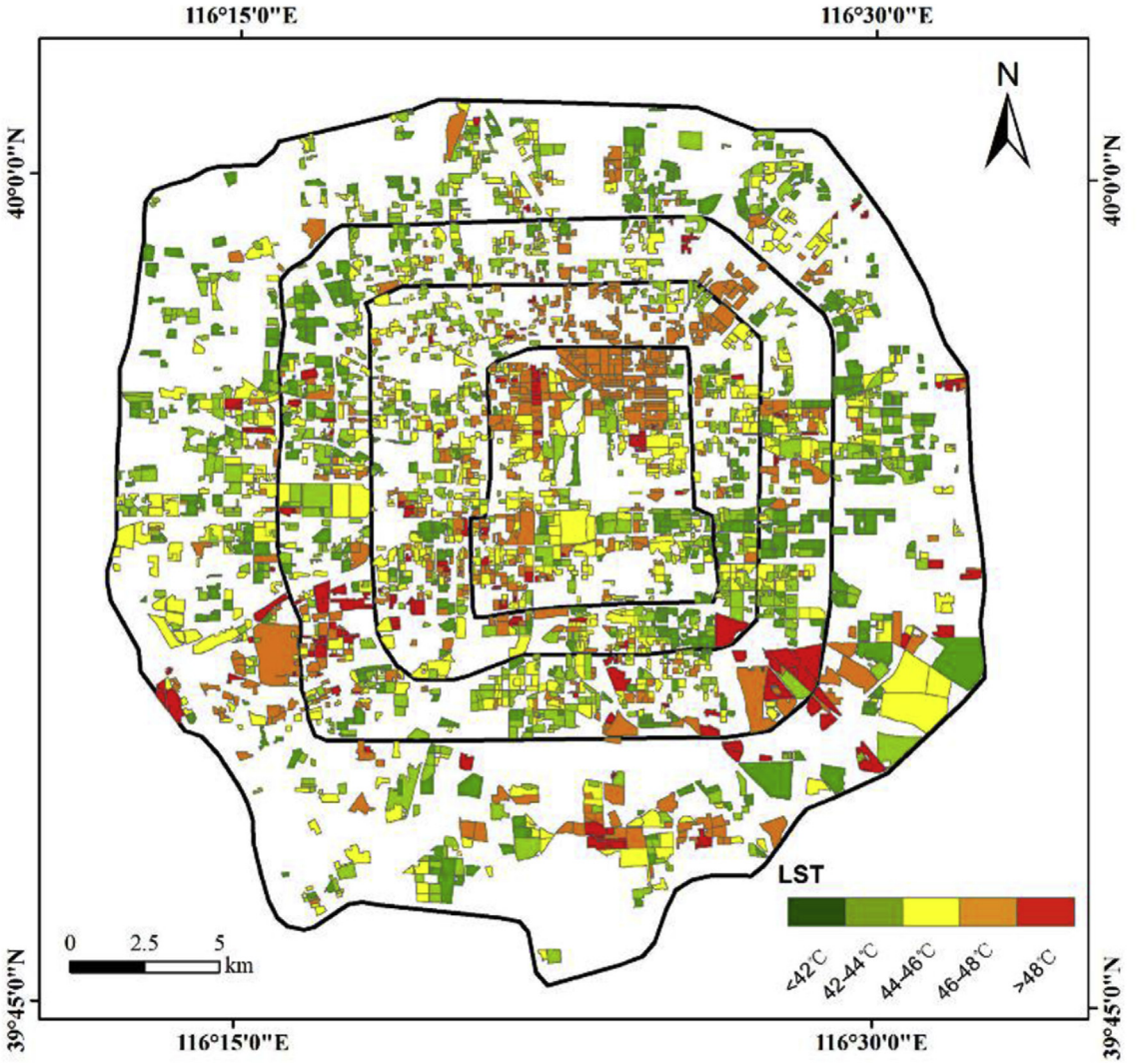

Fig. 3. Land surface temperature of different residential neighborhoods in Beijing.

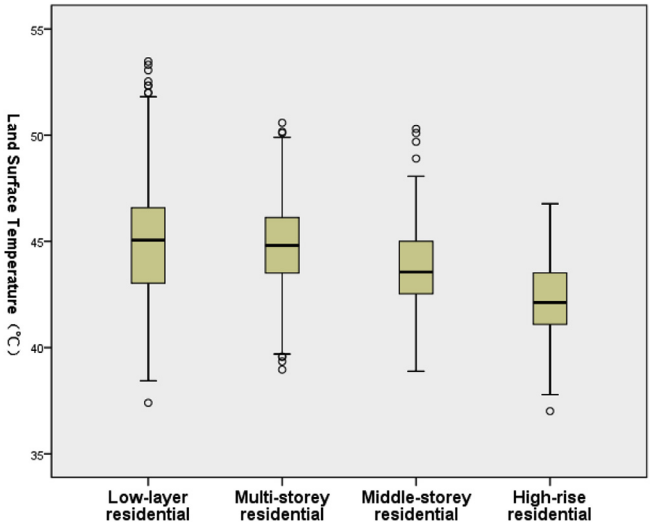

Fig. 4. Mean and variation of LST in the four types of residential neighborhoods in Beijing.

Table 5
Pearson correlations between LST and three variables.

	LST	$\bar{H}$	BD
	−0.42**		
BD	0.41**	−0.24**	
VC	−0.30**	−0.06**	−0.14**

**p < 0.01.

Table 6
Results of regression analysis between LST and three variables.

Variable	Coefficient		Standardized Coefficients	T	Sig.
	B	SE	Beta		
constant	44.724	0.13		342.942	0.000
$\bar{H}$	−0.065	0.003	−0.371	−24.511	0.000
BD	6.217	0.341	0.278	18.229	0.000
VC	−4.069	0.217	−0.278	−18.758	0.000

$R^2 = 0.35$.

density and mean vegetation coverage.

3.2. LST of residential neighborhoods

Land surface temperature varied greatly among residential neighborhoods (Fig. 3), ranging from 53.5 °C to 37.0 °C, with a mean of 44.2 °C and a standard deviation of 2.4 °C. Residential neighborhoods with relatively high LST clustered within the 2nd-ring road, and were located near the southeastern and southwestern corners of the 4th-ring road. Residential neighborhoods with relatively low LST were mainly distributed in the northwest and eastern portions of Beijing. Mean LST in residential neighborhoods decreased slightly from the 2nd-ring road to the 5th-ring road.

High-rise residential neighborhoods had the lowest LST, and mean LST decreased from low-rise to high-rise residential neighborhoods (Table 3), and values were significantly different among the four types of residential neighborhoods (Table 4). Paired comparison tests further showed that LST of multi-story residential neighborhoods was significantly higher than that of mid-rise residential neighborhoods, which was significantly higher than that of high-rise residential neighborhoods (Table 4). However, the difference in LST between low-rise and multi-story residential neighborhoods was not significant. In addition, large variations of LST also occurred within residential neighborhoods of the same type (Fig. 4 and Table 3). For example, LST of low-rise residential neighborhoods ranged from 37.4 °C to 53.5 °C, with standard deviation of 2.8 °C.

3.3. Effects of building height, building density, and vegetation coverage on LST, and their relative importance

Pearson's correlation analysis showed that building height, building density, and percent coverage of vegetation were all significantly correlated with LST (Table 5). Mean building height and vegetation coverage had negative correlations with LST, indicating that LST decreases with an increasing of mean height and vegetation coverage in residential neighborhoods. However, building density was positively correlated with LST. After controlling for the effects of building density and vegetation coverage, the partial correlation between LST and mean height of residential neighborhoods was −0.407 ($p < 0.01$).

Results from the regression analysis showed that all three variables had significant effects on LST. Among the three variables, building height was the most important variable in predicting LST, as suggested by the standardized regression coefficients of the predictors (Table 6). The magnitudes of the two variables, building density and vegetation coverage, were similar. The three variables jointly explained 35.2% of the total variation in LST.

4. Discussion

4.1. Effect of building height on LST

Our results showed that building height had significantly negative effects on LST in residential neighborhoods, even after controlling for the effects of building density and vegetation cover. Residential neighborhoods with higher buildings tend to have lower LST. Previous studies that considered the effects of building height on temperature have mostly focused on the effects of urban geometry, particularly the height/width (H/W) ratio on air temperature (Shashua-Bar et al., 2004; Andreou and Axarli, 2012; Lau et al., 2015). Studies have found that an increase of H/W ratio, that is, a deeper street canyon, generally leads to lower daytime air temperature, but higher night-time air temperature (Oke et al., 1991; Arnfield, 2003). In contrast, there is much less research on the relationship between building height and LST, and the results from these studies are inconsistent. Some studies indicated that higher buildings lead to higher LST around them (e.g.,Yang and Li, 2015; Guo et al., 2016). But other scholars found that building height have negative effects on LST, that is, higher buildings are associated with lower LST (e.g., Cai et al., 2018). Former studies have different results because they ignored other landscape metrics having effect on LST. Actually, Vegetation coverage and building density often changed with height of building increasing, and both of them have significantly effects on LST (Table .3). By consideration of vegetation cover and building density, we found building height had significantly negative effect on LST.

Land surface temperature is directly affected, and thereby the result of surface energy balances and surface net radiation (Oke, 1981; Xiao et al., 2008; Kuang et al., 2015). Buildings decrease the net solar radiation reached the land surfaces by blocking the solar radiation. The higher the buildings, the larger the shaded areas they generate, and then potentially, greater areas of lower LST. Consequently, higher buildings in the residential neighborhood lead to lower LST.

4.2. The relative importance of building height, density, and vegetation cover on LST in residential neighborhood

Our results showed that all the three variables, building height, building density, and vegetation cover, had significant effects on LST. In particular, building height was the most important factor affecting LST

at residential neighborhood, among the three variables. Previous studies have largely focused on the effects of percent coverage of vegetation and impervious surfaces on LST (Zhou et al., 2011; Li et al., 2012). Our results highlight the importance of the vertical structure, such as the building height on LST.

In our results, building height had more significant effects on LST than building density and vegetation cover. Such result is different from some previous studies, which indicated that vegetation cover is the most important factor on LST (e.g.,Xiao et al., 2008; Guo et al., 2015). Such difference may be due to the different unit of analysis. This study was conducted at the residential neighborhood scale, with relative small size of unit, and very mixed buildings and vegetation. Vegetation patches at such scale tend to be highly fragmented and very small (Qian et al., 2015; Zhou et al., 2018). Consequently, shadow provided by trees is frequently overlapped with that caused by buildings. Additionally, such small and highly fragmented greenspaces may not generate significant cool island effect (Zhang et al., 2009; Cao et al., 2010; Li et al., 2013). Therefore, greenspaces in residential neighborhoods tend to have much less effects on LST compared with buildings. This also partially explained the phenomena observed in this study that residential neighborhood with taller building have less vegetation had lower LST. Whether other functional zones (e.g., industrial, commercial) with taller buildings would have lower LST warrants further studies.

Results from this study showed that the increase in building height can significantly reduce LST in residential neighborhoods. Furthermore, we found high-rise residential neighborhoods have a much lower building density than others, which decreases LST further (Zhou et al., 2011; Cai and Xu, 2017) and provides more space for greening. The results have important implications for urban design and planning, particularly for cities where urbanization is still in process. Development in the vertical dimension (i.e., high-rise apartments) has the potential to reduce the planar building density, and thus increase greenspace coverage, leading to cooler residential neighborhoods.

5. Summary and conclusions

This study investigates the variation of LST in residential neighborhoods with different building heights, and further examines the effects of building height, building density and vegetation coverage on LST, and their relative importance. The results show that LST varied greatly among residential neighborhoods, and high-rise residential neighborhoods had the lowest LST. Building height, building density and vegetation coverage all significantly affect LST, and building height is the most significant factor affecting LST, suggesting building height is the most dominant variable affecting LST in residential neighborhoods. While the underlying mechanisms warrant further studies, this result may suggest that in addition to the many other socioeconomic benefits of high-rise residential buildings (Forman, 2014), high-rise residential areas may have advantages in cooling. Whether other functional zones (e.g., industrial, commercial) with taller buildings would have lower LST warrants further studies. Additionally, cross-city comparisons and investigation on seasonal variations (Zhou et al., 2014)are also highly desirable.

Acknowledgment

This research was funded by the National Natural Science Foundation of China (Grant No. 41422104, 41590841, 41601180, and 41771203).

Appendix A. Supplementary data

Supplementary data to this article can be found online at https://doi.org/10.1016/j.pce.2019.01.008.

References

Akbari, H., Pomerantz, M., Taha, H., 2001. Cool surfaces and shade trees to reduce energy use and improve air quality in urban areas. Sol. Energy 70, 295–310.
Amiri, R., Weng, Q., Alimohammadi, A., Alavipanah, S.K., 2009. Spatial–temporal dynamics of land surface temperature in relation to fractional vegetation cover and land use/cover in the Tabriz urban area, Iran. Remote Sens. Environ. 113, 2606–2617.
Andreou, E., Axarli, K., 2012. Investigation of urban canyon microclimate in traditional and contemporary environment. Experimental investigation and parametric analysis. Renew. Energy 43, 354–363.
Antrop, M., 2004. Landscape change and the urbanization process in Europe. Landsc. Urban Plann. 67, 9–26.
Arnfield, A.J., 2003. Two decades of urban climate research: a review of turbulence, exchanges of energy and water, and the urban heat island. Int. J. Climatol. 23, 1–26.
Barsi, J.A., Schott, J.R., Palluconi, F.D., Helder, D.L., Hook, S.J., Markham, B.L., Chander, G., O"Donnell, E.M., 2003. Landsat TM and ETM+ thermal band calibration. Can. J. Remote Sens. 29, 141–153.
Basu, R., Ostro, B., 2008. A multicounty analysis identifying the populations vulnerable to mortality associated with high ambient temperature in California. Am. J. Epidemiol. 168, 632–637.
Beijing Municipal Statistics Bureau, 2013. Statistic Yearbook of Beijing. China Statistics Press, Beijing.
Berger, C., Rosentreter, J., Voltersen, M., Baumgart, C., Schmullius, C., Hese, S., 2017. Spatio-temporal analysis of the relationship between 2D/3D urban site characteristics and land surface temperature. Remote Sens. Environ. 193, 225–243.
Cai, H., Xu, X., 2017. Impacts of built-up area expansion in 2D and 3D on regional surface temperature. Sustainability 9, 1862.
Cai, Z., Han, G., Chen, M., 2018. Do water bodies play an important role in the relationship between urban form and land surface temperature? Sustain. Cities.Soc. 39.
Cao, X., Onishi, A., Chen, J., Imura, H., 2010. Quantifying the cool island intensity of urban parks using ASTER and IKONOS data. Landsc. Urban Plann. 96, 224–231.
Chun, B., Guldmann, J.M., 2014. Spatial statistical analysis and simulation of the urban heat island in high-density central cities. Landsc. Urban Plann. 125, 76–88.
Dubayah, R.O., Drake, J.B., 2000. Lidar remote sensing for forestry. J. For. 98 (43), 44–46.
Duneier, M., 2006. Ethnography, the ecological fallacy, and the 1995 chicago heat wave. Am. Sociol. Rev. 71, 679–688.
Forman, R.T.T., 1995. Land mosaics. The ecology of landscapes and regions. Proc. Sca 201–208.
Forman, R.T.T., 2014. Urban Ecology: Science of Cities. Cambridge University Press, Cambridge.
Gal, T., Unger, J., 2009. Detection of ventilation paths using high-resolution roughness parameter mapping in a large urban area. Build. Environ. 44, 198–206.
Giridharan, R., Lau, S.S.Y., Ganesan, S., 2005. Nocturnal heat island effect in urban residential developments of Hong Kong. Energy Build. 37, 964–971.
Golany, G.S., 1996. Urban design morphology and thermal performance. Atmos. Environ. 30, 455–465.
Grimmond, S., 2007. Urbanization and global environmental change: local effects of urban warming. Geogr. J. 173, 83–88.
Guhathakurta, S., Gober, P., 2007. The impact of the phoenix urban heat island on residential water use. J. Am. Plann. Assoc. 73, 317–329.
Guo, G., Wu, Z., Xiao, R., Chen, Y., Liu, X., Zhang, X., 2015. Impacts of urban biophysical composition on land surface temperature in urban heat island clusters. Landsc. Urban Plann. 135, 1–10.
Guo, G., Zhou, X., Wu, Z., Xiao, R., Chen, Y., 2016. Characterizing the impact of urban morphology heterogeneity on land surface temperature in Guangzhou, China. Environ. Model. Softw 84, 427–439.
Hsieh, C.M., Huang, H.C., 2016. Mitigating urban heat islands: a method to identify potential wind corridor for cooling and ventilation. Comput. Environ. Urban Syst. 57, 130–143.
Jiao, M., Zhou, W., Zheng, Z., Wang, J., Qian, Y., 2017. Patch size of trees affects its cooling effectiveness: a perspective from shading and transpiration processes. Agric. For. Meteorol. 247, 293–299.
Kuang, W., Liu, Y., Dou, Y., Chi, W., Chen, G., Gao, C., Yang, T., Liu, J., Zhang, R., 2015. What are hot and what are not in an urban landscape: quantifying and explaining the land surface temperature pattern in Beijing, China. Landsc. Ecol. 30, 357–373.
Lau, K.L., Lindberg, F., Rayner, D., Thorsson, S., 2015. The effect of urban geometry on mean radiant temperature under future climate change: a study of three European cities. Int. J. Biometeorol. 59, 799–814.
Lee, T., Kim, T., 2013. Automatic building height extraction by volumetric shadow analysis of monoscopic imagery. Int. J. Rem. Sens. 34, 5834–5850.
Li, X., Zhou, W., Ouyang, Z., 2013. Relationship between land surface temperature and spatial pattern of greenspace: what are the effects of spatial resolution? Landsc. Urban Plann. 114, 1–8.
Li, X., Zhou, W., Ouyang, Z., Xu, W., Zheng, H., 2012. Spatial pattern of greenspace affects land surface temperature: evidence from the heavily urbanized Beijing metropolitan area, China. Landsc. Ecol. 27, 887–898.
Liu, M., Hu, Y.-M., Li, C.-L., 2017. Landscape metrics for three-dimensional urban building pattern recognition. Appl. Geogr. 87, 66–72.
Matsumoto, Fumiaki, Fujibe, Hideo, Takahashi, 2017. Urban climate in the Tokyo metropolitan area in Japan. J. Environ. Sci. 59, 54–62.
Ministry of Construction of the People's Republic of China, 2005a. Chinese Residential Building Code. China Architecture & Building Press.
Ministry of Construction of the People's Republic of China, 2005b. Code for Design of Civil Buildings. China Architecture & Building Press.

Naughton, M.P., Henderson, A., Mirabelli, M.C., Kaiser, R., Wilhelm, J.L., Kieszak, S.M., Rubin, C.H., Mcgeehin, M.A., 2002. Heat-related mortality during a 1999 heat wave in Chicago. Am. J. Prev. Med. 22, 221–227.
Nichol, J.E., 1996. High-resolution surface temperature patterns related to urban morphology in a tropical city: a satellite-based study. J. Appl. Meteorol. 35, 135–146.
Oke, T.R., 1981. Canyon geometry and the nocturnal urban heat island: comparison of scale model and field observations. J. Climatol. 1, 237–254.
Oke, T.R., 1988. Street design and urban canopy layer climate. Energy Build. 11, 103–113.
Oke, T.R., 1995. The heat island of the urban boundary layer - characteristics, causes and effects. In: Cermak, J.E., Davenport, A.G., Plate, E.J., Viegas, D.X. (Eds.), Wind Climate in Cities, pp. 81–107.
Oke, T.R., Johnson, G.T., Steyn, D.G., Watson, I.D., 1991. Simulation of surface urban heat islands under 'ideal' conditions at night part 2: diagnosis of causation. Boundary-Layer Meteorol. 56, 339–358.
Oleson, K.W., Bonan, G.B., Feddema, J., Jackson, T., 2011. An examination of urban heat island characteristics in a global climate model. Int. J. Climatol. 31, 1848–1865.
Qian, Y., Zhou, W., Li, W., Han, L., 2015. Understanding the dynamic of greenspace in the urbanized area of Beijing based on high resolution satellite images. Urban For. Urban Green. 14, 39–47.
Qiao, Z., Tian, G.J., Zhang, L.X., Xu, X.L., 2014. Influences of urban expansion on urban heat island in Beijing during 1989-2010. Advan. Meteorol. 11.
Seto, K.C., Fragkias, M., Guneralp, B., Reilly, M.K., 2011. A meta-analysis of global urban land expansion. PLoS One 6.
Shashua-Bar, L., Swaid, H., Hoffman, M.E., 2004. On the correct specification of the analytical CTTC model for predicting the urban canopy layer temperature. Energy Build. 36, 975–978.
Su, W., Zhang, Y., Yang, Y., Ye, G., 2014. Examining the impact of greenspace patterns on land surface temperature by coupling LiDAR data with a CFD model. Sustainability 6, 6799–6814.
Sun, S., Salvaggio, C., 2013. Aerial 3D building detection and modeling from airborne LiDAR point clouds. IEEE J. Select. Topic. Appl. Earth Obs. Remote Sens. 6, 1440–1449.
Unger, J., 2006. Modelling of the annual mean maximum urban heat island using 2D and 3D surface parameters. Clim. Res. 30, 215–226.
Voogt, J.A., Oke, T.R., 2003. Thermal remote sensing of urban climates. Remote Sens. Environ. 86, 370–384.
Wu, J., 2009. Urban sustainability: an inevitable goal of landscape research. Landsc. Ecol. 25, 1–4.
Xiao, R., Ouyang, Z., Li, W., Zhang, Z., Wang, X., 2007. Spatial-temporal distribution and causes of urban heat islands. Scientia Meteorologlca Sinica 27, 230–236.
Xiao, R., Weng, Q., Ouyang, Z., Li, W., Schienke, E.W., Zhang, Z., 2008. Land surface temperature variation and major factors in Beijing, China. Photogramm. Eng. Rem. Sens. 74, 451–461.
Yan, W.Y., Shaker, A., El-Ashmawy, N., 2015. Urban land cover classification using airborne LiDAR data: a review. Remote Sens. Environ. 158, 295–310.
Yang, X., Li, Y., 2015. The impact of building density and building height heterogeneity on average urban albedo and street surface temperature. Build. Environ. 90, 146–156.
Zhang, X.Y., Zhong, T.Y., Feng, X.Z., Ke, W., 2009. Estimation of the relationship between vegetation patches and urban land surface temperature with remote sensing. Int. J. Rem. Sens. 30, 2105–2118.
Zhao, Q., Myint, S.W., Wentz, E.A., Fan, C., 2015. Rooftop surface temperature analysis in an urban residential environment. Rem. Sens. 7, 12135–12159.
Zhou, W., 2013. An object-based approach for urban land cover classification: integrating LiDAR height and intensity data. IEEE Geosci. Remote Sens. Lett. 10, 928–931.
Zhou, W., Huang, G., Cadenasso, M.L., 2011. Does spatial configuration matter? Understanding the effects of land cover pattern on land surface temperature in urban landscapes. Landsc. Urban Plann. 102, 54–63.
Zhou, W., Pickett, S.T.A., Cadenasso, M.L., 2017a. Shifting concepts of urban spatial heterogeneity and their implications for sustainability. Landsc. Ecol. 1–16.
Zhou, W., Qian, Y., Li, X., Li, W., Han, L., 2014. Relationships between land cover and the surface urban heat island: seasonal variability and effects of spatial and thematic resolution of land cover data on predicting land surface temperatures. Landsc. Ecol. 29, 153–167.
Zhou, W., Troy, A., Grove, M., 2008. Object-based land cover classification and change analysis in the Baltimore metropolitan area using multitemporal high resolution remote sensing data. Sensors 8, 1613–1636.
Zhou, W., Wang, J., Cadenasso, M.L., 2017b. Effects of the spatial configuration of trees on urban heat mitigation: a comparative study. Remote Sens. Environ. 195, 12.
Zhou, W., Wang, J., Qian, Y., Pickett, S.T., Li, W., Han, L., 2018. The rapid but "invisible" changes in urban greenspace: a comparative study of nine Chinese cities. Sci. Total Environ. 627, 1572–1584.